Astron. Astrophys. 57, 193—198 (1977)

ASTRONOMY AND ASTROPHYSICS

Acoustic Waves in the Solar Atmosphere

II. Radiative Damping

W. Kalkofen[1] and P. Ulmschneider[2]

[1] Center for Astrophysics, 60 Garden Street, Cambridge, Mass. 02138, USA
[2] Institut für Astrophysik, Am Hubland, D-8700 Würzburg, Federal Republic of Germany

Received July 19, revised October 29, 1976

Summary. In this second of a series of papers studying large amplitude acoustic waves, we consider the calculation of the entropy change due to emission and absorption of radiation. We develop a method for the numerical solution of the equation of radiative transfer for atmospheres in which shock discontinuities may occur. As an illustration of our numerical method we construct a radiative equilibrium model of a stellar atmosphere by solving the time-dependent equations.

Key words: radiative transfer — radiative damping — acoustic waves

I. Introduction

In this second paper (Paper II) of a series exploring the behavior of acoustic waves in the solar atmosphere we show how radiation is included in the hydrodynamic code described by Ulmschneider et al. (1977, called henceforth Paper I).

In previous research, the transfer equation has usually been solved approximately either in the diffusion or optically thin limit. For example, Vincenti and Baldwin (1962) studied the propagation of acoustic waves of small amplitude in a radiating gas with the diffusion approximation for the radiative transfer, and Christy (1964) used the diffusion approximation while solving the non-linear hydrodynamic equations. Hill (1972) extended this work to include transfer in a grey gas in the Eddington approximation. Radiation transfer was treated without making these approximations by Cannon (1974), Klein et al. (1976) and Kneer and Nakagawa (1976) in studies of shock wave propagation in an atmosphere of one-level atoms in statistical equilibrium. They solved the time-dependent hydrodynamic equations with finite difference methods rather than the method of characteristics (cf. Paper I) and treated the radiative damping with differential equation methods. In addition, these authors allowed for departures from local thermodynamic equilibrium (LTE). We restrict our computations to the photosphere and low chromosphere. Vernazza et al. (1976) have shown that up to the temperature minimum at optical depth $\tau_{5000}=5E-5$ the departure coefficient b_{H^-} of H^- is very close to unity. For radially propagating acoustic waves the main contribution to radiative damping arises in the depth range $\tau_{5000}=10$ to 0.01, and we feel that the simplifying assumption of LTE is a very good approximation in the treatment of this process.

The method we describe in this paper is based on integral equations (Kalkofen, 1974). We derive the basic radiation expressions to be used with the time-dependent hydrodynamic equations, describe the numerical solution of the transfer equation, and consider approximations valid in limiting cases. We then test the numerical solution against an exact solution and indicate the range of validity of the approximate expressions. Finally we combine the transfer equation with the hydrodynamic equations to construct a model atmosphere in radiative equilibrium.

Send offprint requests to: P. Ulmschneider

II. Radiative Damping

Equation (25) of Paper I requires the specification of the entropy change per unit time due to gains and losses of photons in an element of mass. Let dS be the entropy increase per gram and dQ the amount of energy per cm^3 gained by a net influx of photons into the gas element. We may then write

$$\left.\frac{dS}{dt}\right|_{\text{Rad}} = \frac{1}{\varrho T}\left.\frac{dQ}{dt}\right|_{\text{Rad}}. \tag{1}$$

The notation used here is the same as in Paper I. The increase in thermal energy dQ is provided by a decrease of the radiative flux πF,

$$\left.\frac{dQ}{dt}\right|_{\text{Rad}} = -\frac{\partial \pi F}{\partial x}, \tag{2}$$

where x is the geometrical height coordinate pointing vertically out of the sun. The flux πF is computed from

the equation of radiative transfer (Sampson, 1965, p. 25),

$$\frac{\partial I_\nu}{c_L \partial t} + \mu \frac{\partial I_\nu}{\partial x} = -\varkappa_\nu (I_\nu - S_\nu), \tag{3}$$

where I_ν is the intensity, S_ν the source function, $\varkappa_\nu$ the absorption coefficient and c_L the velocity of light. Integrating Equation (3) over angle and frequency leads to the radiative energy equation

$$\frac{4\pi}{c_L}\frac{\partial J}{\partial t} + \frac{\partial \pi F}{\partial x} = -4\pi \int_0^\infty \varkappa_\nu (J_\nu - S_\nu) d\nu . \tag{4}$$

Multiplying Equation (3) by μ/c_L and integrating over angle and frequency we obtain the radiative momentum equation,

$$\frac{1}{c_L^2}\frac{\partial \pi F}{\partial t} + \frac{\partial P_r}{\partial x} = \frac{1}{c_L}\int_0^\infty \varkappa_\nu \pi F_\nu d\nu . \tag{5}$$

Here J_ν, J are the mean intensities, $\pi F_\nu, \pi F$ radiation fluxes and P_r the radiation pressure.

The energy and momentum Equations (4) and (5) augment the hydrodynamic equations of Paper I (Sampson, 1965, p. 33). In the solar atmosphere the derivative of the energy density $4\pi J/c_L$ and of the radiation pressure P_r may be neglected. The ratio of the energy density term to the emission term on the right hand side of Equation (4) is approximately equal to

$$\frac{4\pi/c_L \Delta B/\frac{1}{2}P}{4\pi\varkappa \Delta B} = \frac{2}{c_L \varkappa P} \approx 10^{-5}, \tag{6}$$

where $P = 25$ s is the period of a typical wave and $\varkappa = 2E-7\,\mathrm{cm}^{-1}$ is the absorption coefficient near optical depth unity. Similarly, the ratio of the radiation pressure to the gas pressure perturbation is in the range

$$\frac{\Delta p_r}{\Delta p} = \frac{4\pi \Delta B}{3c_L \Delta p} = \frac{16\sigma T^3 \Delta T}{3c_L \Delta p} \approx 10^{-5} \text{ to } 10^{-3} \tag{7}$$

for typical values $\Delta p = 7\mathrm{E}3\,\mathrm{dyn/cm}^2$, $\Delta T = 30$ K near $\tau = 1$ and $\Delta p = 150\,\mathrm{dyn/cm}^2$, $\Delta T = 300$ K near $\tau = 10^{-4}$. B is the integrated Planck function. Under the assumption of LTE in the solar photosphere and low chromosphere the radiative damping function D may therefore be written as

$$D \equiv \left.\frac{dS}{dt}\right|_{\mathrm{Rad}} = \frac{4\pi}{\varrho T}\int_0^\infty \varkappa_\nu (J_\nu - B_\nu) d\nu , \tag{8}$$

where B_ν is the Planck function.

III. Approximations

In optically thick and in thin regions the flux derivative of Equation (4) may be computed from approximate expressions. At large optical depth, $\tau_\nu \gg 1$, we make the Eddington approximation and write Equation (4)

$$\frac{d\pi F}{dx} = -4\pi \int_0^\infty \varkappa_\nu \frac{1}{3}\frac{d^2 J_\nu}{d\tau_\nu^2} d\nu . \tag{9}$$

This is the diffusion approximation.

Since far from the boundary $J_\nu \approx B_\nu$, Equation (9) may also be written as

$$\frac{d\pi F}{dx} = -4\pi \int_0^\infty \varkappa_\nu \frac{1}{3}\frac{d^2 B_\nu}{d\tau_\nu^2} d\nu . \tag{10}$$

The mean intensity J_ν at the surface may be regarded as originating from optical depth $\tau_\nu = 1$. Thus, near the surface, where $\tau_\nu \ll 1$, the mean intensity is practically constant. The energy Equation (4) may therefore be written as

$$\frac{\partial \pi F}{\partial x} \approx -4\pi \int_0^\infty \varkappa_\nu (J_\nu(0) - S_\nu) d\nu , \tag{11}$$

where $J_\nu(0)$ is the surface value of the mean intensity. The approximations (9)–(11) are useful in tests of the numerical procedure.

IV. Numerical Treatment

The calculation of the radiative damping function D of Equation (8) from a prescribed source function S_ν requires three numerical integrations: the τ-integration for the specific intensities I_ν^+ and I_ν^-, the angle integration for the mean intensity J_ν, and the frequency integration in Equation (8). Of these, the μ and ν integrations are straight forward with a Gaussian integration scheme (Abramowitz and Stegun, 1964, p. 887). The τ-integration is more complicated, because the source function S_ν is given at a fixed height grid and not at positions determined by an integration scheme. Consequently care is required in the interpolation of the S_ν's. Moreover, since the τ-integration involves many exponentials whose computation is time consuming, this integration must be treated with care.

1) The τ-integration

We assume that the source function S_ν is given at a finite set of depth points x_i $(i = 1, N)$,

$$S_i = S_\nu(x_i, \mu) \tag{12}$$

and is allowed to depend on angle. This x-grid corresponds to a τ-grid

$$\tau_i = \frac{\tau_\nu(x_i)}{|\mu|}. \tag{13}$$

For the numerical integration of the source function a parabolic expansion recommends itself because it leads to the diffusion approximation at large depth, a feature that is important for flux conservation.

2) Outward Radiation $I^+(\mu > 0)$

For the set of discrete τ-points we write the transfer equation as

$$I_i^+ = \sum_{k=i}^{N-1} \int_{\tau_k}^{\tau_{k+1}} S^+(t) e^{-(t-\tau_i)} dt + I_N^+ e^{-(t_N - \tau_i)}, \tag{14}$$

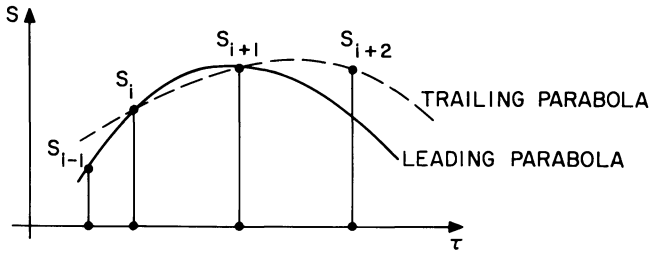

Fig. 1. Approximation of the source function by leading or trailing parabolas for the computation of I_i^+

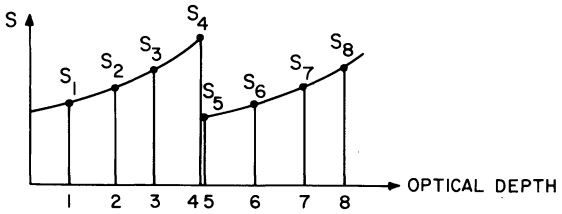

Fig. 2. Source function jump near a shock wave

where $I_i^+ = I_\nu^+(\tau_i)$.

This equation suggests that we compute the intensities I_i^+ recursively.

For the parabolic expansion of the source function in the interval $\tau_i \leqq t \leqq \tau_{i+1}$ we write

$$S^+(t) = S_i^+ + (t-\tau_i)S' + (t-\tau_i)^2 S''. \tag{15}$$

Since the contribution of the source term S_i^+ is usually large we improve accuracy by subtracting this term:

$$\begin{aligned} I_i^+ - S_i^+ = {} & (I_{i+1}^+ - S_{i+1}^+)e^{-\delta} + (S_{i+1}^+ - S_i^+)e^{-\delta} \\ & + S'[1-(1+\delta)e^{-\delta}] \\ & + S''[2-(2+2\delta+\delta^2)e^{-\delta}], \end{aligned} \tag{16}$$

where

$$\delta_k^1 \equiv \tau_1 - \tau_k\,; \quad \delta \equiv \delta_i^{i+1}. \tag{17}$$

The values S' and S'' are determined by the requirement that Equation (15) be satisfied at three neighboring grid points.

The integration interval $(i, i+1)$ is spanned (see Fig. 1) by a parabola passing through the points $(i-1, i, i+1)$, the leading parabola in the integration for the outward intensity I^+, and a parabola passing through $(i, i+1, i+2)$, the trailing parabola.

At large depth the diffusion approximation holds: The value of the mean intensity J_ν is equal to that of the source function S_ν up to a term proportional to the second derivative of S_ν with respect to optical depth. Deep in the atmosphere, where the source function becomes a linear function of optical depth, the mean intensity becomes equal to the source function. There the net radiative heating and the entropy change vanish. It is necessary that the numerical integration of the transfer equation reproduce the diffusion limit faithfully. Otherwise a spurious energy source or sink results, which can set a static atmosphere in motion (see Paper I). To ensure that the diffusion limit is reproduced, the same parabola must be used for both the inward and the outward directed intensities. This is achieved when the intensities I^+ and I^- at point i are both calculated with their respective leading parabolas, except when i refers to a boundary point or a shock point where trailing parabolas have to be used.

We use the notation:

$$\Delta \equiv \delta_{i-2}^{i-1}\,; \quad \delta_- \equiv \delta_{i-1}^{i}\,; \quad \delta \equiv \delta_i^{i+1}\,; \quad \delta_+ \equiv \delta_{i+1}^{i+2}. \tag{18}$$

Evaluating S' and S'' for the leading parabola we find

$$\begin{aligned} I_i^+ - S_i^+ = {} & (I_{i+1}^+ - S_{i+1}^+)e^{-\delta} + S_{i-1}^+ PM \\ & + S_i^+ PO + S_{i+1}^+ PP, \end{aligned} \tag{19}$$

where

$$\begin{aligned} PM &= \frac{1}{\delta_-(\delta+\delta_-)}[2-\delta-(2+\delta)e^{-\delta}] \\ &\approx \frac{\delta^3}{2\delta_-(\delta+\delta_-)} \\ &\quad \cdot \left[-1+\frac{1}{3}\left(1-\frac{\delta}{4}\left(1-\frac{\delta}{5}\left(1-\frac{\delta}{6}\right)\right)\right)(2+\delta)\right], \end{aligned} \tag{20}$$

$$\begin{aligned} PO &= \frac{1}{\delta\delta_-}[\delta-\delta_- -2+(\delta+\delta_-+2)e^{-\delta}] \\ &\approx -1+\frac{\delta}{2}\left(1+\frac{\delta}{\delta_-}\right)-\frac{\delta^2}{6\delta_-} \\ &\quad \cdot \left[1-\frac{\delta}{4}\left(1-\frac{\delta}{5}\left(1-\frac{\delta}{6}\right)\right)\right](\delta+\delta_-+2), \end{aligned} \tag{21}$$

and

$$\begin{aligned} PP &= \frac{1}{\delta(\delta+\delta_-)}[\delta_- +2-(2+2\delta+\delta_-)e^{-\delta}] \\ &\approx 1-\frac{\delta}{2}\left(1+\frac{\delta}{\delta+\delta_-}\right)+\frac{\delta^2}{6(\delta+\delta_-)} \\ &\quad \cdot \left[1-\frac{\delta}{4}\left(1-\frac{\delta}{5}\left(1-\frac{\delta}{6}\right)\right)\right](2+2\delta+\delta_-). \end{aligned} \tag{22}$$

When the optical distances δ and δ_- become very short, the three lowest orders in δ or δ_- of Equation (20) and the two lowest orders in Equations (21) and (22) cancel. To avoid a loss of accuracy we use the expansions whenever δ becomes smaller than 10^{-2}.

For an expansion of the source function S^+ using the trailing parabola, the solution for the outward intensity is

$$\begin{aligned} I_i^+ - S_i^+ = {} & (I_{i+1}^+ - S_{i+1}^+)e^{-\delta} + S_i^+ RM \\ & + S_{i+1}^+ RO + S_{i+2}^+ RP, \end{aligned} \tag{23}$$

where

$$RM=\frac{1}{\delta(\delta+\delta_+)}[2-2\delta-\delta_+-(2-\delta_+)e^{-\delta}]$$
$$\approx-\frac{1}{(\delta+\delta_+)}\left[\delta_++(2-\delta_+)\frac{\delta}{2}\cdot\left(1-\frac{\delta}{3}\left(1-\frac{\delta}{4}\left(1-\frac{\delta}{5}\left(1-\frac{\delta}{6}\right)\right)\right)\right)\right], \quad (24)$$

$$RO=\frac{1}{\delta\delta_+}[\delta+\delta_+-2+(2+\delta-\delta_+)e^{-\delta}]$$
$$\approx\frac{1}{\delta_+}\left[\delta_+-\delta+(2+\delta-\delta_+)\frac{\delta}{2}\cdot\left(1-\frac{\delta}{3}\left(1-\frac{\delta}{4}\left(1-\frac{\delta}{5}\left(1-\frac{\delta}{6}\right)\right)\right)\right)\right], \quad (25)$$

$$RP=\frac{1}{\delta_+(\delta+\delta_+)}[2-\delta-(2+\delta)e^{-\delta}]$$
$$\approx-\frac{\delta^3}{2\delta_+(\delta+\delta_+)}\left\{1-\frac{1}{3}(2+\delta)\cdot\left[1-\frac{\delta}{4}\left(1-\frac{\delta}{5}\left(1-\frac{\delta}{6}\right)\right)\right]\right\}. \quad (26)$$

3) Inward Radiation $I_i^-(\mu\leqq 0)$

For the inward intensity we write

$$I_i^-=\sum_{k=2}^{i}\int_{\tau_{k-1}}^{\tau_k}S^-(t)e^{-(\tau_i-t)}dt. \quad (27)$$

Again we calculate I_i^- recursively and determine the coefficients S' and S'' by fitting the expansion to the source function at the points $(i-1, i, i+1)$ for the leading parabola and at $(i-2, i-1, i)$ for the trailing parabola.

For the leading parabola, which is used for non-boundary points we have

$$I_i^- - S_i^- = (I_{i-1}^- - S_{i-1}^-)e^{-\delta_-} + S_{i-1}^- QP + S_i^- QO + S_{i+1}^- QM, \quad (28)$$

where QM, QO, QP are obtained from the values PM, PO, PP of Equations (20)–(22) respectively by replacing δ by δ_- and δ_- by δ. For the trailing parabola we find

$$I_i^- - S_i^- = (I_{i-1}^- - S_{i-1}^-)e^{-\delta_-} + S_{i-2}^- TP + S_{i-1}^- TO + S_i^- TM, \quad (29)$$

where TM, TO, TP are obtained from the values RM, RO, RP of Equations (24)–(26) respectively by replacing δ by δ_- and δ_+ by Δ. Here the expansions are used whenever $\delta_-\leqq 10^{-2}$.

4) Boundaries and Shocks

Since we treat the case of zero incident radiation at the upper boundary, the surface boundary condition on the inward intensity is $I_1^-=0$. At the bottom of the atmosphere the outward intensity I_N^+ must be specified.

Near a shock the typical behavior of the source function is given in Figure 2. The Points 1–3 and 6–8 are assumed to be grid points. Points 4 and 5 are on either side of the shock discontinuity such that the distance $\overline{45}$ is infinitesimally small.

The outward intensity I_i^+ may be computed from the boundary up to Point 6 with leading parabolas, using Equation (19), as for an interior point. I_5^+ must be computed with a trailing parabola, using Equation (23). In the preshock region, the outward intensity may again be calculated, with leading parabolas, using the condition

$$I_4^+=I_5^+ \quad (30)$$

at the shock. Similarly, the inward intensity I_i^- may be computed from the surface up to Point 3 with leading parabolas, using Equation (28), and I^- at Point 4 is computed with a trailing parabola, using Equation (29).

With the condition

$$I_5^-=I_4^- \quad (31)$$

at the shock, the intensity at deeper points may again be calculated with leading parabolas.

V. Numerical Tests

The method described in Section IV was tested for a parabolic source function,

$$S^+=S^-=a+b\tau+c\tau^2 \quad (32)$$

for which the analytic solution may be calculated.

As expected, the numerical solution agreed with the analytic result to machine accuracy (12 digits).

In a further test we compared the numerical results with the diffusion and optically thin approximations Equations (9) and (11) in an actual computation of an acoustic wave. The numerical differentiations in this test were performed by a finite difference method. For the diffusion approximation we found better than 5 digit accuracy at $\tau>300$, but only one digit accuracy near $\tau=0.001$. At depths $\tau<0.004$ the diffusion approximation became very poor. The optically thin approximation had a greater than 5 place accuracy for $\tau<5\,10^{-5}$, decreased to about a 1 place accuracy near $\tau=0.03$ and thereafter became rapidly very poor. The τ values here are optical distances along the ray defined by $\mu=1/\sqrt{3}$. The accuracy of the approximations in the range $\tau=0.5$ to 0.001 depends on the phase of the wave.

VI. Radiation Hydrodynamics

Given values of the thermodynamic variables as functions of height we can now use the method described above to compute the radiative damping function as a function of height.

1) Radiative Damping Iteration

As shown in Paper I, to achieve high accuracy the integration of the entropy along the C° characteristics

requires the radiative damping function at the old as well as the new time. The function is known only at the old time, its value at the new time must be determined iteratively. For this calculation a convenient starting estimate is given either by the damping function at the old time or by an extrapolation of the values at several previous times. We found that the solution tends to oscillate about the correct value. To accelerate convergence we averaged the damping function D and the speed of sound c over the current and the previous values at the new time,

$$D=(D_{\text{new}}+D_{\text{prev.}})/2,$$
$$c=(c_{\text{new}}+c_{\text{prev.}})/2. \tag{33}$$

With this procedure, convergence is rapid; we usually needed between 5 and 6 iterations for convergence to 3 significant figures, the limit of accuracy of a trapezoidal integration of D along the C° characteristic.

2) Maximal Entropy Change

In addition to the hydrodynamic time scale, the inclusion of radiation brings another characteristic time scale into the problem. The radiative relaxation time describes the rate of radiative energy or entropy exchange of a fluid element.

To prevent the entropy S of a fluid particle from changing too rapidly due to radiative damping we impose a restriction (like the Courant condition for the hydrodynamic time scale) on the time step whenever the change ΔS becomes too large. Taking the real atmosphere to be locally isothermal with sound velocity c_0 and gravitational acceleration g we find [see Paper I, Eq. (21)] for the allowed maximal entropy change between two adjacent grid points:

$$\Delta S<\frac{\gamma R g}{\mu c_0^2}\frac{H}{10}=\frac{R}{10\mu}. \tag{34}$$

This equation sets a limit for entropy changes independent of gravity. We usually took $\Delta S<2\text{E}6\,\text{erg/g K}$. We found that this condition was less restrictive than the Courant condition except at the start of a calculation when the deviation from radiative equilibrium was greatest.

VI. Radiative Equilibrium Models

As an illustration we use the methods described above to construct a radiative equilibrium atmosphere. In this time-dependent method the surface gravity is incorporated into the characteristic equations while the effective temperature enters as the boundary condition for the incident flux.

We take

$$I_\nu^+(N)=B_\nu(T=5800\,\text{K}) \tag{35}$$

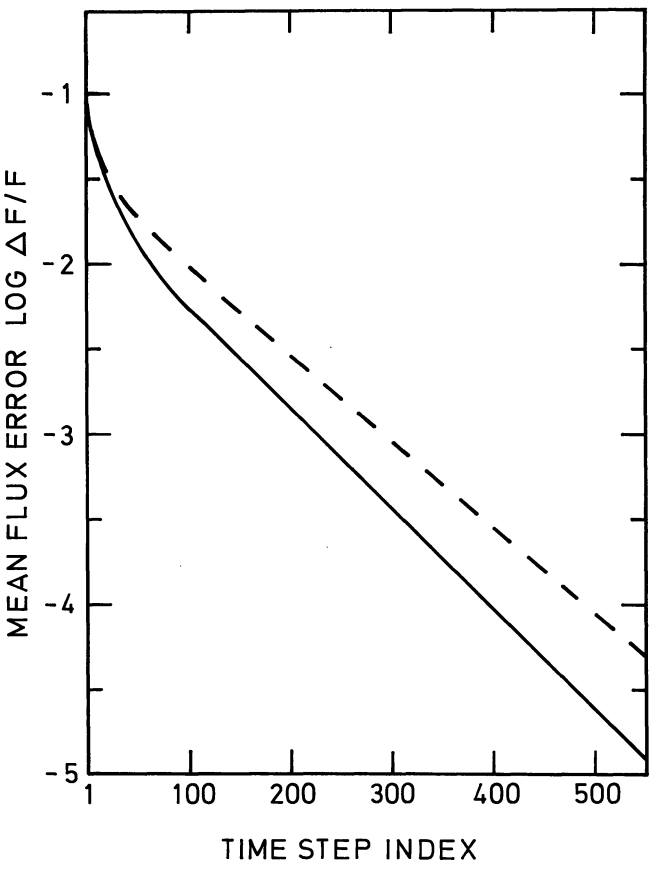

Fig. 3. The mean error of the maximum flux deviation $\Delta F/F$ as function of the time step index. The one frequency point calculation is shown dashed the 10 frequency point calculation is shown drawn

and a solar gravity. To ensure that the atmosphere does not expand we take rigid boundary conditions at the top and bottom.

$$u(1)=u(N)=0. \tag{36}$$

This boundary condition describes the situation of a gas, irradiated from one side enclosed between two transparent plates which are not allowed to move. We start with a linear temperature gradient of $-7\,\text{K/km}$. The temperature at the deepest point was 7000 K and the density $5.0\,\text{E-}7\,\text{g cm}^{-3}$. For opacity sources we used H and H^- as described by Kurucz (1970). The optical depth at the lowest point was 5.6. Two calculations were performed, using one (at 5000 Å) and ten frequency points and taking one angle point at $\mu=1/\sqrt{3}$. The frequencies were spaced at roughly equal intervals up to 1.5 E15 Hz. We took 24 height points covering a distance of 110 km. Figure 3 shows the mean error of the maximum flux deviation at a given time step. It is seen that a 2% accuracy in the flux is reached after about 100 time steps. The flux error decreases by about one order of magnitude every 200 (165) time steps for the 1 (10) frequency point calculation. The scatter of the maximum

flux error around the mean curves in Figure 3 was about a factor of 2. The time step, $\Delta t = 0.53$ s was constant and determined by the Courant condition. The computing time of the 10 frequency point calculation was greater by a factor of 5.

Acknowledgement. We like to thank Dr. L. Cram for reading the manuscript.

References

Abramowitz, M., Stegun, I. A.: 1964, Handbook of math. functions, Nat. Bureau of Standards, Washington
Cannon, C.J.: 1974, *J. Quant. Spectroscop. Radiat. Transfer* **14**, 761
Christy, R.F.: 1964, *Rev. Mod. Phys.* **36**, 555
Gingerich, O., Noyes, R.W., Kalkofen, W., Cuny, Y.: 1971, *Solar Phys.* **18**, 347
Hill, S.J.: 1972, *Astrophys. J.* **178**, 793
Kalkofen, W.: 1974, *Astrophys. J.* **188**, 105
Klein, R.I., Stein, R.F., Kalkofen, W.: 1975, *Astrophys. J.* **205**, 499
Kneer, F., Nakagawa, Y.: 1976, *Astron. Astrophys.* **47**, 65
Kurucz, R.: 1970, SAO Spec. Report **309**
Sampson, D.H.: 1965, Radiative Contribution to Energy and Momentum Transport in a Gas, Interscience, New York
Ulmschneider, P., Kalkofen, W., Nowak, T., Bohn, H.U.: 1977, *Astron. Astrophys.* **54**, 61
Vernazza, J.E., Avrett, E.H., Loeser, R.: 1976, *Astrophys. J. Suppl.* **30**, 1 and private communication
Vincenti, W.G., Baldwin, B.S.: 1962, *J. Fluid. Mech.* **12**, 449
Vincenti, W.G., Krüger, C.H.: 1965, Introduction to Physical Gas Dynamics, Wiley, New York